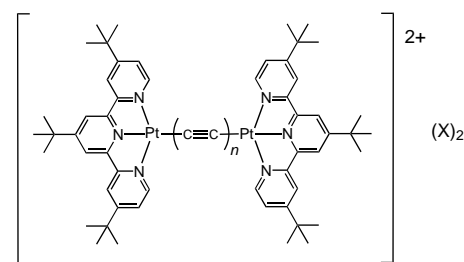


# Luminescent Platinum(II) Terpyridyl-Capped Carbon-Rich Molecular Rods—An Extension from Molecular- to Nanometer-Scale Dimensions\*\*

Vivian Wing-Wah Yam,\* Keith Man-Chung Wong, and Nianyong Zhu

There has been a growing interest in the chemistry of carbon-rich metal-containing systems, in particular those of metal-containing polynes. Examples include the transition-metal end-capped  $[M]-(C\equiv C)_n-[M]$  systems ( $[M] = Re(Cp^*)(NO)-(PPh_3)_3$ ,<sup>[1]</sup> *trans*- $[Pt(C_6F_5)(PR_3)_2]$ ,<sup>[2]</sup>  $Fe(Cp^*)(dppe)_3$ ,<sup>[3]</sup>  $Fe(Cp^*)(CO)_2$ ,<sup>[4]</sup>  $Ru(Cp)(PPh_3)_2$ ,<sup>[5]</sup>  $Mn(dppe)_2$ ,<sup>[6]</sup>  $Re(tBu_2-bpy)(CO)_3$ ,<sup>[7]</sup>  $Au(PCy_3)_3$ ,<sup>[8]</sup>). Some of them have recently been shown to display interesting luminescence behavior.<sup>[7,8]</sup> Despite platinum-containing polynes being known, most of them are confined to platinum phosphane complexes, with corresponding studies on the nitrogen donor analogues unexplored. These, together with the numerous studies on the luminescence behavior of platinum(II)-polypyridine systems,<sup>[9,10]</sup> in particular those of the platinum(II)-terpyridyl complexes,<sup>[9f,10]</sup> and our recent report on the novel solvatochromic properties of platinum(II)-terpyridyl complexes<sup>[11]</sup> as well as our interest in luminescent carbon-rich molecular materials,<sup>[12]</sup> have prompted us to investigate the luminescence properties of the  $[Pt]-(C\equiv C)_n-[Pt]$  system of various alkynyl chain lengths with platinum(II)-terpyridyl groups as the transition-metal end-capped termini. Herein we report the synthesis, electronic absorption, photophysical properties, and structural characterization of a series of alkynyl-bridged dinuclear platinum(II)-terpyridyl complexes,  $[Pt(tBu_3-tpy)-(C\equiv C)_nPt(tBu_3-tpy)](X)_2$  (**1–3**;  $tBu_3-tpy = 4,4',4''$ -tri-*tert*-butyl-2,2':6',2''-terpyridine). The bulky trisubstituted terpyridine ligand was chosen to eliminate the influence of Pt···Pt and  $\pi$ - $\pi$  interactions on the luminescence behavior. The luminescence behavior together with the structure–property relationship of the complexes have been studied.

Figure 1 depicts the structures of the complex cations of **1–3**. In all cases, the platinum(II) metal center adopts an



- 1:  $n = 1$ ,  $X = OTf$   
 2:  $n = 2$ ,  $X = OTf$   
 3:  $n = 4$ ,  $X = PF_6$

essentially square-planar geometry with slight distortion due to the coordination constraints imposed by the terpyridyl ligand (N1–Pt1–N3 160.2–160.4°; N1–Pt1–N2 and N2–Pt1–N3 79.8–80.6°). The two platinum(II)-terpyridyl ends are connected by the alkynyl chain in a linear  $[Pt]-(C\equiv C)_n-[Pt]$  fashion ( $n = 1, 2$ , and 4) with Pt–C angles in the range of 173.8–178.5°. The Pt–C (2.026 Å in **1**; 1.934–1.935 Å in **2** and **3**) and C≡C (1.118 Å in **1**; 1.191–1.210 Å in **2** and **3**) bond lengths are comparable to that found in the related mononuclear counterpart  $[Pt(tBu_3-tpy)(C\equiv C-C\equiv CH)](OTf)^{[11]}$  and in other platinum(II)-alkynyl systems.<sup>[2,10c]</sup> Upon increasing the  $(C\equiv C)_n$  unit, the dimensions of these rigid rodlike complexes are found to extend from the molecular scale to nanoscale; the separation between the two platinum(II) termini ranges from 5.16 Å in **1** to 7.71 Å in **2** and 12.83 Å in **3**. Unlike other related platinum(II) systems, no significant Pt–Pt or  $\pi$ - $\pi$  interaction is observed from the crystal packing of **1–3** owing to the presence of the sterically bulky *tert*-butyl groups on the terpyridyl ligands, which hinder the molecules from coming into close proximity with each other. Similar observations have been reported in other 4,4',4''-tri-*tert*-butyl-2,2':6',2''-terpyridine-containing platinum(II) complexes.<sup>[11]</sup> In contrast to **2** and **3** in which the square planes about the platinum(II)-terpyridyl termini are essentially coplanar, the two platinum(II)-terpyridyl moieties in **1** are twisted with respect to each other with an interplanar angle of 35.83°. This may be rationalized by the fact that the length of the  $C_2$  carbon bridge in **1**, unlike the  $C_4$  and  $C_8$  bridges in **2** and **3**, respectively, is rather short and a slight twisting of the square planes containing the two platinum(II)-terpyridyl units may help to relieve the steric strain arising from the coplanar arrangement of the two adjacent platinum(II)-terpyridyl units.

Complexes **1–3** show intense absorptions at about 308–342 nm and 428–522 nm in acetonitrile at 298 K (Figure 2) and their photophysical data are summarized in Table 1. With reference to previous spectroscopic studies on the mononuclear  $[Pt(tBu_3-tpy)(C\equiv C-C\equiv CH)](OTf)^{[11]}$  and related complexes,<sup>[10]</sup> the high-energy structured absorption bands at about 308–342 nm are ascribed to intra-ligand (IL)  $\pi \rightarrow \pi^*[(C\equiv C)_n]$  and  $\pi \rightarrow \pi^*(tBu_3-tpy)$  transitions of the alkynyl bridge and the substituted terpyridine ligand, while the low-energy band in the visible region is assigned to a  $[d\pi(Pt) \rightarrow \pi^*(tBu_3-tpy)]$  metal-to-ligand charge transfer (MLCT) transition, probably mixed with an  $[\pi(C\equiv C) \rightarrow \pi^*(tBu_3-tpy)]$  alkynyl-to-terpyridine ligand-to-ligand charge transfer

[\*] Prof. V. W.-W. Yam, Dr. K. M.-C. Wong, Dr. N. Zhu  
 Centre for Carbon-Rich Molecular and Nano-Scale Metal-Based  
 Materials Research, Department of Chemistry and  
 HKU-CAS Joint Laboratory on New Materials  
 The University of Hong Kong  
 Pokfulam Road, Hong Kong (P. R. China)  
 Fax: (+852) 2857-1586  
 E-mail: wwyam@hku.hk

[\*\*] V.W.-W.Y. acknowledges support from The University of Hong Kong Foundation for Educational Development and Research Limited, and the receipt of a Croucher Senior Research Fellowship from the Croucher Foundation. This work has been supported by a CERG Grant from the Research Grants Council of Hong Kong Special Administrative Region, China (Project No. HKU 7123/00P). K.M.-C.W. and N.Z. acknowledge the receipt of University Postdoctoral Fellowships from The University of Hong Kong.

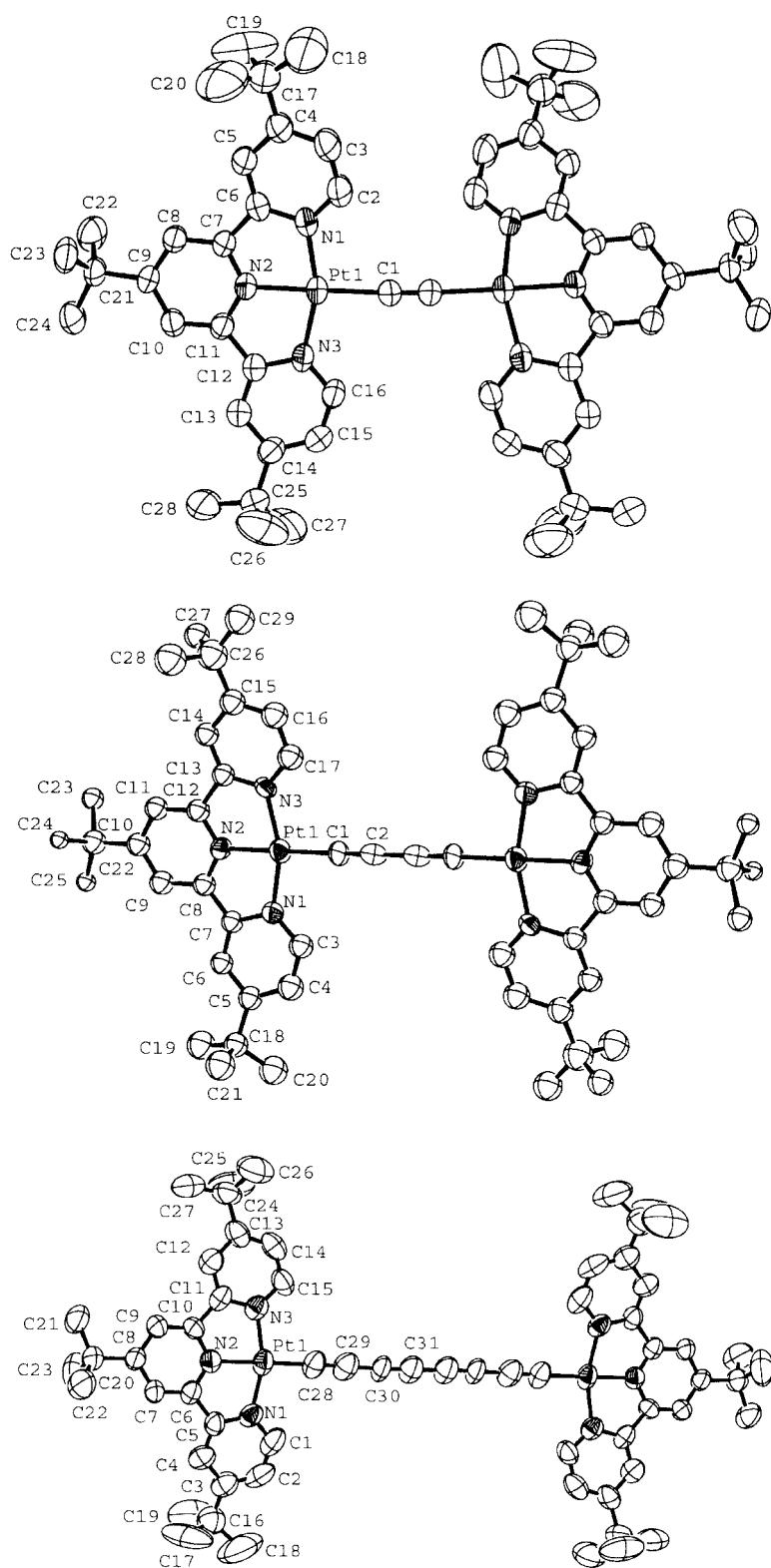


**Figure 1.** Structures of the complex cations of **1** (top), **2** (middle), and **3** (bottom). Hydrogen atoms are omitted for clarity. Thermal ellipsoids are drawn at the 50% probability level.

(LLCT) character. Interestingly, the low-energy absorption band of **2** shows an extinction coefficient that is almost double that of the 382–400 nm band of the related mononuclear

complex,  $[\text{Pt}(\text{tBu}_3\text{-tpy})(\text{C}\equiv\text{C}-\text{C}\equiv\text{CH})](\text{OTf})$ . The low-energy absorption band was found to shift to higher energy upon going from **1** (484–522 nm) to **2** (436–466 nm) and **3** (428–452 nm) with an increasing number of  $\text{C}\equiv\text{C}$  units. This is rather unusual as one would have expected a shift to lower energy with increasing  $\text{C}\equiv\text{C}$  units as is commonly found in organic polyynes<sup>[13]</sup> and in other metal–alkynyl systems.<sup>[8]</sup> The blue shift observed on going from **1** to **2** to **3** is likely to be a result of the greater stabilization of the  $\text{d}\pi$  orbital on platinum(II) upon increasing the length of the conjugated alkynyl chain. Two effects may account for the observed trend. 1) The  $\pi$ -donor ability exhibited by the alkynyl chain, which gives rise to a filled–filled  $\text{p}\pi\text{--d}\pi$  overlap. 2) The  $\pi$ -accepting ability of the alkynyl chain, which results in a  $\text{d}\pi\text{--}\pi^*$  interaction. Given the similar  $\sigma$ -donating ability of the monoyne, diyne, and tetrayne bridges, the  $\pi$ -donor orbital energy of the  $(\text{C}\equiv\text{C})_n$  bridge should follow the order:  $n = 4 > 2 > 1$ . Despite the fact that a better energy match between the  $\text{d}\pi(\text{Pt})$  and the  $\pi(\text{C}\equiv\text{C})_n$  orbitals upon increasing the  $\text{C}\equiv\text{C}$  chain length is expected to raise the  $\text{d}\pi(\text{Pt})$  orbital energy, the decreased overlap integral between the  $\text{d}\pi(\text{Pt})$  and the  $\pi(\text{C}\equiv\text{C})_n$  orbitals resulting from the delocalization of electron density across the  $\text{C}\equiv\text{C}$  unit would, on the other hand, lead to a net overall decrease in the  $\text{d}\pi(\text{Pt})$  orbital energy, rendering the  $\text{d}\pi(\text{Pt})$  orbital on **3**, which has the longest  $(\text{C}\equiv\text{C})_n$  unit, lowest-lying in energy, and hence giving rise to the highest MLCT absorption energy. An alternative rationale arises from the increased  $\pi$ -accepting ability of the alkynyl unit upon increasing the  $(\text{C}\equiv\text{C})_n$  chain, that is, the  $\pi^*(\text{C}\equiv\text{C})_n$  orbital energy follows the order:  $n = 4 < 2 < 1$ , which would stabilize the  $\text{d}\pi(\text{Pt})$  orbital through  $\text{d}\pi\text{--}\pi$  overlap. The higher MLCT energy in **3** is likely to be a result of the greater stabilization of the  $\text{d}\pi(\text{Pt})$  orbital energy. Similar observations have been reported by us in the related rhenium(I)–alkynyl system.<sup>[12f]</sup>

Upon excitation at  $\lambda > 400$  nm, **1–3** both in the solid state and in solution exhibit intense luminescence at about 550–625 nm (Table 1). With reference to the spectroscopic studies on other platinum(II)–terpyridyl systems<sup>[10]</sup> and the occurrence of the emission at similar energies to that found in the related mononuclear complex  $[\text{Pt}(\text{tBu}_3\text{-tpy})(\text{C}\equiv\text{C}-\text{C}\equiv\text{CH})](\text{OTf})$ ,<sup>[11]</sup> the origin of the luminescence is assigned as derived from states of predominantly  $^3\text{MLCT}$  [ $\text{d}\pi(\text{Pt}) \rightarrow \pi^*(\text{tBu}_3\text{-tpy})$ ] character, probably mixed with some intraligand  $^3\text{IL}$  [ $\pi \rightarrow \pi^*(\text{C}\equiv\text{C})_n$ ], and ligand-to-ligand charge transfer  $^3\text{LLCT}$  [ $\pi(\text{C}\equiv\text{C})_n \rightarrow \pi^*(\text{tBu}_3\text{-tpy})$ ] character. The excitation spectra of **1–3** (Figure 3a) show excitation bands at about 425–525 nm, which closely resemble that of the low-energy MLCT bands in

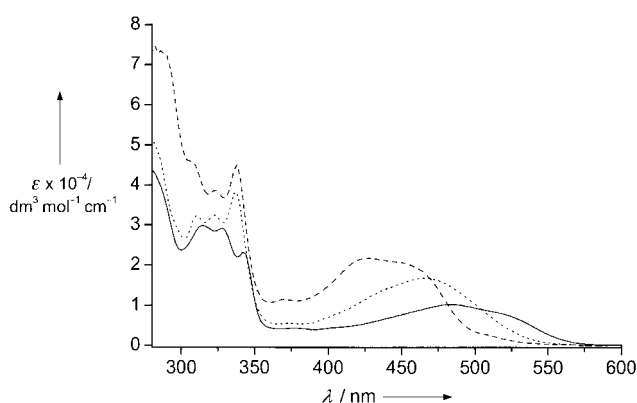


**Figure 2.** Electronic absorption spectra of **1** (—), **2** (.....), and **3** (-----) in acetonitrile at room temperature.

**Table 1:** Photophysical data for **1**–**3**.

Complex	Medium (T [K])	Absorption $\lambda_{\text{max}}$ [nm] ( $\epsilon_{\text{max}}$ [dm <sup>3</sup> mol <sup>−1</sup> cm <sup>−1</sup> ])	Emission $\lambda_{\text{max}}$ [nm] ( $\tau_{\text{o}}$ [μs])
<b>1</b>	MeCN (298)	314 (29820), 328 (29180), 342 (23155), 484 (10175), 522 (7615)	625
	solid (298)		615 (0.2)
	solid (77)		604 (2.6) {1270} <sup>[a]</sup>
	glass (77)		572 (8.1) {1250} <sup>[a]</sup>
<b>2</b>	MeCN (298)	310 (32210), 322 (32475), 338 (38110), 436 (13510), 466 (16670)	625
	solid (298)		606 (0.2)
	solid (77)		604 (1.1) {1270} <sup>[a]</sup>
	glass (77)		550 (6.5) {1230} <sup>[a]</sup>
<b>3</b>	MeCN (298)	308 (45705), 324 (38590), 338 (44980), 428 (21690), 452 (20480)	589 {2050} <sup>[a]</sup>
	solid (298)		605 (0.2) {2020} <sup>[a]</sup>
	solid (77)		607 (1.0) {2060} <sup>[a]</sup>
	glass (77)		582 (1.1) {2100} <sup>[a]</sup>

[a] Vibrational progressional spacings [cm<sup>−1</sup>].

their respective electronic absorption spectra, further supportive of an assignment of a <sup>3</sup>MLCT band mixed with some of <sup>3</sup>IL/<sup>3</sup>LLCT character. The emission band of **3** is vibronically structured with vibrational progressional spacings of about 2052 cm<sup>−1</sup>; such spacings are typical of a  $\nu(\text{C}\equiv\text{C})$  stretch in the ground state. This observation indicates the involvement of the alkynyl bridge, and the possible mixing of a <sup>3</sup>LLCT

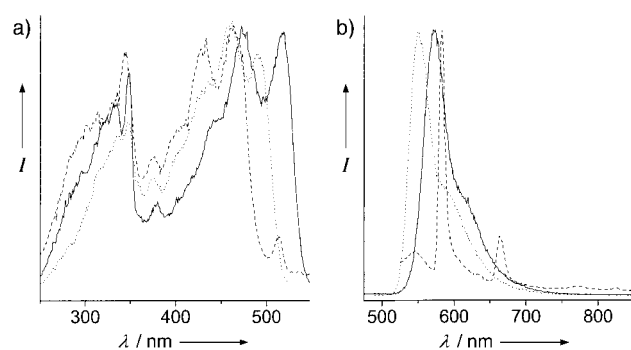


**Figure 3.** a) Excitation and b) emission spectra of **1** (—), **2** (.....), and **3** (-----) in butyronitrile at 77 K. *I* = normalized emission intensity.

$[\pi(\text{C}\equiv\text{C})_n \rightarrow \pi^*(t\text{Bu}_3\text{-tpy})]$  state and an <sup>3</sup>IL [ $\pi \rightarrow \pi^*(\text{C}\equiv\text{C})_n$ ] state into the <sup>3</sup>MLCT [ $d\pi(\text{Pt}) \rightarrow \pi^*(t\text{Bu}_3\text{-tpy})$ ] character. Similarly, the emission spectra of **1** and **2** in glass at 77 K exhibit vibronically structured bands with vibrational progressional spacings of about 1250 cm<sup>−1</sup>, typical of the  $\nu(\text{C}\equiv\text{C})$  and  $\nu(\text{C}\equiv\text{N})$  stretching modes of the terpyridyl ligand. It is likely that the origin of the emission has in addition to a <sup>3</sup>MLCT origin, mixing of a <sup>3</sup>LLCT and <sup>3</sup>IL character, with the mixing being more important in **3** with the increasing  $\pi$  conjugation in the C<sub>8</sub> chain. The observation of a Huang–Rhys factor of less than 1 in the emission spectra of **1** and **2** in butyronitrile glass at 77 K is in line with an assignment of predominantly <sup>3</sup>MLCT character. Similar to that observed in the electronic absorption spectroscopy, a blue shift of the emission band was observed upon going from **1** (572 nm) to **2** (550 nm) in butyronitrile glass at 77 K (Figure 3b). Argu-

ments similar to that discussed for the trend in the electronic absorption energy have been made to explain the observed trend in the emission energies of **1** and **2**. On the other hand, the emission spectrum of **3** in butyronitrile glass at 77 K shows a vibronically structured emission band at about 582 nm with vibrational progressional spacings of about 2100 cm<sup>−1</sup>, typical of the  $\nu(\text{C}\equiv\text{C})$  stretch in the ground state. It is likely that upon increasing the  $\pi$  conjugation of the C<sub>n</sub> chain, the origin of the emission changes in character, with an increasing contribution from the <sup>3</sup>IL [ $\pi \rightarrow \pi^*(\text{C}\equiv\text{C})_n$ ] excited state, leading to an emission that is predominantly <sup>3</sup>IL in character.

## Experimental Section

Complexes **1** and **2** were synthesized by the reaction of [Pt(*t*Bu<sub>3</sub>-tpy)(MeCN)](OTf)<sub>2</sub> with TMS-C≡CH and TMS-C≡C-C≡C-TMS, respectively, in the presence of KF in methanol. Orange-red crystals of **1** and **2** were obtained from an *n*-hexane/acetonitrile mixture after column chromatography on silica gel by using dichloromethane–acetone as eluent. Complex **3** was prepared by the oxidative coupling reaction of [Pt(*t*Bu<sub>3</sub>-tpy)(C≡C-C≡CH)](OTf)<sub>2</sub> in the presence of a catalytic amount of copper(II) acetate in pyridine. Metathesis reaction with NH<sub>4</sub>PF<sub>6</sub>, followed by column chromatography on silica gel, and recrystallization from slow diffusion of *n*-hexane into a solution of **3** in dichloromethane yielded the pure forms of **3** as orange-red crystals.

**1:** <sup>1</sup>H NMR (400 MHz, CD<sub>3</sub>CN, 298 K, relative to Me<sub>4</sub>Si):  $\delta$  = 9.36 (d with Pt satellites, 4H; terpyridyl H), 8.48 (s, 4H; terpyridyl H), 8.42 (d, 4H; terpyridyl H), 7.78 (dd, 4H; terpyridyl H), 1.58 (s, 18H; *tert*-butyl H), 1.48 ppm (s, 36H; *tert*-butyl H); <sup>13</sup>C NMR (125.8 MHz, CD<sub>3</sub>CN, 298 K, relative to Me<sub>4</sub>Si):  $\delta$  = 167.6, 167.5, 160.1, and 55.3 (quaternary C on terpyridine), 154.9, 126.7, 124.1, and 122.3 (tertiary C on terpyridine), 113.4 (Pt–C), 38.1 and 37.1 (quaternary C on *tert*-butyl group), 30.7 and 30.4 ppm (primary C on *tert*-butyl group); positive ESI-MS: *m/z* 1365 [*M*–OTf]<sup>+</sup>, 609 [*M*–2OTf]<sup>2+</sup>; elemental analyses calcd (%) for C<sub>58</sub>H<sub>70</sub>F<sub>6</sub>N<sub>6</sub>O<sub>6</sub>PtS<sub>2</sub>·1.5CH<sub>2</sub>Cl<sub>2</sub>: C 43.50, H 4.45, N 5.12; found: C 43.50, H 4.50, 5.16.

**2:** <sup>1</sup>H NMR (400 MHz, CD<sub>3</sub>CN, 298 K, relative to Me<sub>4</sub>Si):  $\delta$  = 9.04 (d with Pt satellites, 4H; terpyridyl H), 8.36 (s, 4H; terpyridyl H), 8.32 (d, 4H; terpyridyl H), 7.80 (dd, 4H; terpyridyl H), 1.54 (s, 18H; *tert*-butyl H), 1.46 ppm (s, 36H; *tert*-butyl H); <sup>13</sup>C NMR (125.8 MHz,

CD<sub>3</sub>CN, 298 K, relative to Me<sub>4</sub>Si):  $\delta$  = 168.5, 168.1, 159.9, and 155.3 (quaternary C on terpyridine), 155.0, 127.0, 124.4, and 122.5 (tertiary C on terpyridine), 91.1 (Pt–C≡C–), 87.4 (Pt–C≡C–), 38.1 and 37.2 (quaternary C on *tert*-butyl group), 30.6 and 30.3 ppm (primary C on *tert*-butyl group); positive ESI-MS:  $m/z$  1389 [M–OTf]<sup>+</sup>, 620 [M–2OTf]<sup>2+</sup>; elemental analyses calcd (%) for C<sub>60</sub>H<sub>70</sub>F<sub>6</sub>N<sub>6</sub>O<sub>6</sub>Pt<sub>2</sub>S<sub>2</sub>·CH<sub>2</sub>Cl<sub>2</sub>: C 45.10, H 4.44, N 5.18; found: C 45.36, H 4.48, N 5.01.

**3:** <sup>1</sup>H NMR (400 MHz, CD<sub>3</sub>CN, 298 K, relative to Me<sub>4</sub>Si):  $\delta$  = 8.84 (d with Pt satellites, 4H; terpyridyl H), 8.36 (s, 4H; terpyridyl H), 8.32 (d, 4H; terpyridyl H), 7.76 (dd, 4H; terpyridyl H), 1.54 (s, 18H; *tert*-butyl H), 1.46 ppm (s, 36H; *tert*-butyl H); <sup>13</sup>C NMR (125.8 MHz, CD<sub>3</sub>CN, 298 K, relative to Me<sub>4</sub>Si):  $\delta$  = 169.4, 168.6, 159.7 and 155.4 (quaternary C on terpyridine), 154.8, 127.2, 124.6 and 122.7 (tertiary C on terpyridine), 97.2 (Pt–C≡C–C≡C–), 87.1 (Pt–C≡C–C≡C–), 64.5 (Pt–C≡C–C≡C–), 59.3 ppm (Pt–C≡C–C≡C–); positive ESI-MS:  $m/z$  1434 [M–PF<sub>6</sub>]<sup>+</sup>, 645 [M–2PF<sub>6</sub>]<sup>2+</sup>; elemental analyses calcd for C<sub>62</sub>H<sub>70</sub>F<sub>12</sub>N<sub>6</sub>P<sub>2</sub>Pt<sub>2</sub>: C 47.15, H 4.44, N 5.32; found: C 47.19, H 4.41, N 4.94.

Crystal data for **1**·(C<sub>2</sub>H<sub>5</sub>)<sub>2</sub>O: C<sub>58</sub>H<sub>70</sub>F<sub>6</sub>N<sub>6</sub>O<sub>6</sub>Pt<sub>2</sub>S<sub>2</sub>·C<sub>4</sub>H<sub>10</sub>O;  $M_r$  = 1589.62, crystal dimensions 0.4 × 0.1 × 0.05 mm<sup>3</sup>, monoclinic, space group C2/c,  $a$  = 24.224(5),  $b$  = 17.755(4),  $c$  = 16.529(3) Å,  $\beta$  = 108.25(3)°,  $V$  = 6751(2) Å<sup>3</sup>,  $Z$  = 4,  $\rho_{\text{calcd}}$  = 1.564 g cm<sup>−3</sup>,  $\mu(\text{MoK}\alpha)$  = 4.271 mm<sup>−1</sup>,  $F(000)$  = 3168,  $T$  = 293 K;  $R$  = 0.0308,  $wR$  = 0.0756 for 5435 reflections with  $I > 2\sigma(I)$ . MAR diffractometer, MoK $\alpha$  radiation ( $\lambda$  = 0.71073 Å); collection range  $2\theta_{\text{max}}$  = 50.69° with 2° oscillation step of  $\varphi$ , 420 s exposure time and scanner distance at 120 mm; 88 images were collected. For **2**·2(CH<sub>3</sub>)<sub>2</sub>CO: C<sub>60</sub>H<sub>70</sub>F<sub>6</sub>N<sub>6</sub>O<sub>6</sub>Pt<sub>2</sub>S<sub>2</sub>·2C<sub>3</sub>H<sub>6</sub>O;  $M_r$  = 1655.68, crystal dimensions 0.2 × 0.1 × 0.02 mm<sup>3</sup>, monoclinic, space group P2<sub>1</sub>/c,  $a$  = 16.348(3),  $b$  = 10.540(2),  $c$  = 20.594(4) Å,  $\beta$  = 92.72(3)°,  $V$  = 3544.5(12) Å<sup>3</sup>,  $Z$  = 2,  $\rho_{\text{calcd}}$  = 1.551 g cm<sup>−3</sup>,  $\mu(\text{MoK}\alpha)$  = 4.072 mm<sup>−1</sup>,  $F(000)$  = 1652,  $T$  = 301 K;  $R$  = 0.0489,  $wR$  = 0.1088 for 3837 reflections with  $I > 2\sigma(I)$ . MAR diffractometer, MoK $\alpha$  radiation ( $\lambda$  = 0.71073 Å); collection range  $2\theta_{\text{max}}$  = 49.82° with 2° oscillation step of  $\varphi$ , 1200 s exposure time and scanner distance at 120 mm; 53 images were collected. For **3**·4(CH<sub>3</sub>)<sub>2</sub>CO: C<sub>62</sub>H<sub>70</sub>F<sub>12</sub>N<sub>6</sub>P<sub>2</sub>Pt<sub>2</sub>·4C<sub>3</sub>H<sub>6</sub>O;  $M_r$  = 1811.67, crystal dimensions 0.3 × 0.1 × 0.05 mm<sup>3</sup>, monoclinic, space group C2<sub>1</sub>/c,  $a$  = 14.220(3),  $b$  = 14.158(3),  $c$  = 20.329(4) Å,  $\beta$  = 95.44(3)°,  $V$  = 4074.3(14) Å<sup>3</sup>,  $Z$  = 2,  $\rho_{\text{calcd}}$  = 1.477 g cm<sup>−3</sup>,  $\mu(\text{MoK}\alpha)$  = 3.544 mm<sup>−1</sup>,  $F(000)$  = 1812,  $T$  = 301 K;  $R$  = 0.0403,  $wR$  = 0.0916 for 4637 reflections with  $I > 2\sigma(I)$ . MAR diffractometer, MoK $\alpha$  radiation ( $\lambda$  = 0.71073 Å); collection range  $2\theta_{\text{max}}$  = 50.66° with 2° oscillation step of  $\varphi$ , 900 s exposure time and scanner distance at 120 mm; 80 images were collected. CCDC-198503 (**1**·(C<sub>2</sub>H<sub>5</sub>)<sub>2</sub>O), CCDC-198504 (**2**·2(CH<sub>3</sub>)<sub>2</sub>CO), and CCDC-198505 (**3**·4(CH<sub>3</sub>)<sub>2</sub>CO) contain the supplementary crystallographic data for this paper. These data can be obtained free of charge via [www.ccdc.cam.ac.uk/conts/retrieving.html](http://www.ccdc.cam.ac.uk/conts/retrieving.html) (or from the Cambridge Crystallographic Data Centre, 12, Union Road, Cambridge CB2 1EZ, UK; fax: (+44) 1223-336-033; or deposit@ccdc.cam.ac.uk).

Received: November 25, 2002 [Z50627]

**Keywords:** alkynes · luminescence · molecular rods · N ligands · platinum

Hampel, J. A. Gladysz, *Angew. Chem.* **2002**, *114*, 1951; *Angew. Chem. Int. Ed.* **2002**, *41*, 1871.

- [3] a) F. Paul, C. Lapinte, *Coord. Chem. Rev.* **1998**, *178–180*, 431; b) N. Le Narvor, C. Lapinte, *J. Chem. Soc. Chem. Commun.* **1993**, 357; c) N. Le Narvor, L. Toupet, C. Lapinte, *J. Am. Chem. Soc.* **1995**, *117*, 7129.
- [4] M. Akita, M. C. Chung, A. Sakurai, S. Sugimoto, M. Terada, M. Tanaka, Y. Moro-oka, *Organometallics* **1997**, *16*, 4882.
- [5] a) M. I. Bruce, *Coord. Chem. Rev.* **1997**, *166*, 91; b) M. I. Bruce, P. J. Low, K. Costuas, J. F. Halet, S. P. Best, G. A. Heath, *J. Am. Chem. Soc.* **2000**, *122*, 1949.
- [6] S. Kheradmandan, K. Heinze, H. W. Schmalke, H. Berke, *Angew. Chem.* **1999**, *111*, 2412; *Angew. Chem. Int. Ed.* **1999**, *38*, 2270.
- [7] a) V. W. W. Yam, *Chem. Commun.* **2001**, 789; b) V. W. W. Yam, V. C. Y. Lau, K. K. Cheung, *Organometallics* **1995**, *14*, 2749; c) V. W. W. Yam, V. C. Y. Lau, K. K. Cheung, *Organometallics* **1996**, *15*, 1740.
- [8] a) C. M. Che, H. Y. Chao, V. M. Miskowski, Y. Li, K. K. Cheung, *J. Am. Chem. Soc.* **2001**, *123*, 4985; b) W. Lu, H. F. Xiang, N. Zhu, C. M. Che, *Organometallics* **2002**, *21*, 2343.
- [9] a) *Extended Linear Chain Compounds* (Ed.: J. S. Miller), Plenum, New York, **1982**; b) D. M. Roundhill, H. B. Gray, C. M. Che, *Acc. Chem. Res.* **1989**, *22*, 55; c) V. H. Miskowski, V. H. Houlding, *Coord. Chem. Rev.* **1991**, *111*, 145; d) C. W. Chan, L. K. Cheng, C. M. Che, *Coord. Chem. Rev.* **1994**, *132*, 87; e) H. Yersin, D. Donges, *Top. Curr. Chem.* **2001**, *214*, 82; f) D. R. McMillin, J. J. Moore, *Coord. Chem. Rev.* **2002**, *229*, 113.
- [10] a) J. A. Bailey, M. G. Hill, R. E. Marsh, V. M. Miskowski, W. P. Schaefer, H. B. Gray, *Inorg. Chem.* **1995**, *34*, 4591; b) R. Büchner, C. T. Cunningham, J. S. Field, R. J. Haines, D. R. McMillin, G. C. Summerton, *J. Chem. Soc. Dalton Trans.* **1999**, 711; c) V. W. W. Yam, R. P. L. Tang, K. M. C. Wong, K. K. Cheung, *Organometallics* **2001**, *20*, 4476.
- [11] V. W. W. Yam, K. M. C. Wong, N. Zhu, *J. Am. Chem. Soc.* **2002**, *124*, 6506.
- [12] a) V. W. W. Yam, *Acc. Chem. Res.* **2002**, *35*, 555; b) V. W. W. Yam, K. K. W. Lo, K. M. C. Wong, *J. Organomet. Chem.* **1999**, *578*, 3; c) V. W. W. Yam, K. K. W. Lo, *Chem. Soc. Rev.* **1999**, *28*, 323; d) V. W. W. Yam, K. L. Cheung, L. H. Yuan, K. M. C. Wong, K. K. Cheung, *Chem. Commun.* **2000**, 1513; e) V. W. W. Yam, S. H. F. Chong, C. C. Ko, K. K. Cheung, *Organometallics* **2000**, *19*, 5092.
- [13] a) R. Eastmond, T. R. Johnson, D. R. M. Walton, *Tetrahedron* **1972**, *28*, 4601; b) G. Schermann, T. Grösser, F. Hampel, A. Hirsch, *Chem. Eur. J.* **1997**, *3*, 1105.

[1] a) R. Dembinski, B. Bartik, T. Bartik, M. Jaeger, J. A. Gladysz, *J. Am. Chem. Soc.* **2000**, *122*, 810; b) W. E. Meyer, A. J. Amoroso, C. R. Horn, M. Jaeger, J. A. Gladysz, *Organometallics* **2001**, *20*, 1115.

[2] a) T. B. Peters, J. C. Bohling, A. M. Arif, J. A. Gladysz, *Organometallics* **1999**, *18*, 3261; b) W. Mohr, J. Stahl, F. Hampel, J. A. Gladysz, *Inorg. Chem.* **2001**, *40*, 3263; c) J. Stahl, J. C. Bohling, E. B. Bauer, T. B. Peters, W. Mohr, J. M. Martín-Alvarez, F.